Splice isoform and pharmacological studies reveal that sterol depletion relocalizes α-synuclein and enhances its toxicity

Julie S. Valastyan[a,b], Daniel J. Termine[a], and Susan Lindquist[a,b,c,1]

[a]Whitehead Institute for Biomedical Research, Cambridge, MA 02142; [b]Department of Biology, Massachusetts Institute of Technology, Cambridge, MA 02139; and [c]Howard Hughes Medical Institute, Massachusetts Institute of Technology, Cambridge, MA 02139

Contributed by Susan Lindquist, December 31, 2013 (sent for review July 29, 2013)

Synucleinopathies are neurodegenerative diseases associated with toxicity of the lipid-binding protein α-synuclein (α-syn). When expressed in yeast, α-syn associates with membranes at the endoplasmic reticulum and traffics with vesicles out to the plasma membrane. At higher levels it elicits a number of phenotypes, including blocking vesicle trafficking. The expression of α-syn splice isoforms varies with disease, but how these isoforms affect protein function is unknown. We investigated two of the most abundant isoforms, resulting in deletion of exon four (α-synΔ4) or exon six (α-synΔ6). α-SynΔ4, missing part of the lipid-binding domain, had reduced toxicity and membrane binding. α-SynΔ6, missing part of the protein–protein interaction domain, had reduced toxicity but no reduction in membrane binding. To compare the mechanism by which the splice isoforms exert toxicity, equally toxic strains were probed with genetic modifiers of α-syn–induced toxicity. Most modifiers equally altered the toxicity induced by the splice isoforms and full-length α-syn (α-synFL). However, the splice isoform strains responded differently to a sterol-binding protein, leading us to examine the effect of sterols on α-syn–induced toxicity. Upon inhibition of sterol synthesis, α-synFL and α-synΔ6, but not α-synΔ4, showed decreased plasma membrane association, increased vesicular association, and increased cellular toxicity. Thus, higher membrane sterol concentrations favor plasma membrane binding of α-synFL and α-synΔ6 and may be protective of synucleinopathy progression. Given the common use of cholesterol-reducing statins and these potential effects on membrane binding proteins, further investigation of how sterol concentration and α-syn splice isoforms affect vesicular trafficking in synucleinopathies is warranted.

Alpha synuclein (α-syn) is a 14-kDa protein associated with progression of synucleinopathies, a family of neurodegenerative diseases that includes Parkinson's disease (PD), multiple system atrophy, and dementia with Lewy bodies (1). Each of these diseases is characterized by the degeneration of diverse neuronal subtypes or of oligodendrocytes. The accumulation of misfolded α-syn is a hallmark of all these diseases. Moreover, increased expression of α-syn (through copy number variation or the effects of regulatory SNPs) can cause these diseases (2–4). Indeed, many laboratories now model synucleinopathies by overexpressing α-syn (5–7).

The structural properties of α-syn provide insight into its biology. Its N terminus is composed of seven imperfect repeats that fold into amphipathic helices in the presence of lipids, allowing α-syn to interact with membranes (8). α-Syn also can form toxic multimers, a property dependent on amino acids 71–82 (9). Finally, the protein contains an unstructured C-terminal tail important for various protein–protein interactions (10). These basic biophysical properties affect α-syn functionality, allowing much simpler cell types, such as yeast, to be used in modeling α-syn–induced cellular pathologies. Indeed, studying the cell biology of α-syn in *Saccharomyces cerevisiae* affords multiple advantages (11). Yeast share with higher organisms fundamental eukaryotic cell biology, including mitochondria, peroxisomes, vesicular trafficking, protein homeostasis, autophagy, and other functions of direct relevance to disease. Moreover, yeast provide an unparalleled genetic toolbox, enabling both detailed hypothesis-driven analyses and unbiased screen-based discovery.

When α-syn is expressed at low levels in yeast, it localizes to the plasma membrane, highlighting its lipophilic nature. In both yeast and neurons, α-syn associates with lipid rafts, suggesting that α-syn displays similar lipid-binding preferences in both cell types. The exact composition of α-syn's preferred lipid environment is not understood; however, current work suggests that α-syn is sensitive both to the type of lipids and how they are packed into the bilayer (12, 13).

α-Syn reaches the plasma membrane by associating with vesicles formed in the endoplasmic reticulum (ER) and trafficking throughout the secretory pathway. The process of vesicular fusion with a target membrane in yeast and synaptic vesicle fusion in neurons is highly conserved and uses many similar proteins, including v-SNAREs, t-SNAREs, synaptobrevin, NSF, and Rab GTPases (14). Much of what now is known about these processes was discovered first in yeast and later applied to cells of higher organisms, including neurons. In yeast, however, secretion is constitutive, allowing vesicles to fuse with the plasma membrane without an external signal (15). In neurons, in contrast, presynaptic vesicles fuse with the plasma membrane in a controlled manner.

At higher expression levels, α-syn reduces trafficking of vesicles through the secretory pathway and forms foci at the sites where vesicles accumulate (5). This observation, first discovered in yeast and later verified in mammalian neurons, is in keeping with α-syn's role in helping regulate secretion of presynaptic

Significance

The small, lipid-binding protein, α-synuclein (α-syn), is associated with neurodegenerative diseases. α-Syn exists in various splice isoforms, and isoform expression varies with disease, but how these isoforms affect protein function is unknown. Using a yeast model expressing α-syn splice variants, we show that inhibition of sterol synthesis differentially affects α-syn plasma membrane association, vesicular association, and cellular toxicity, depending on which α-syn isoform is expressed. This result suggests that higher membrane sterol concentrations may be protective of synucleinopathy progression. Given the common use of cholesterol-reducing statins and their potential effects on membrane-binding proteins, further investigation of how sterol concentration and α-syn splice isoforms affect vesicular trafficking in synucleinopathies is warranted.

Author contributions: J.S.V., D.J.T., and S.L. designed research; J.S.V. and D.J.T. performed research; J.S.V. contributed new reagents/analytic tools; J.S.V., D.J.T., and S.L. analyzed data; S.L. supervised and directed the overall project; and J.S.V. and S.L. wrote the paper.

The authors declare no conflict of interest.

[1]To whom correspondence should be addressed. E-mail: lindquist_admin@wi.mit.edu.

This article contains supporting information online at www.pnas.org/lookup/suppl/doi:10.1073/pnas.1324209111/-/DCSupplemental.

vesicles (16). Higher expression in yeast also elicits a number of cellular defects, including slowed growth, lipid droplet accumulation, release of reactive oxygen species, and mitochondrial dysfunction (5, 17, 18). Importantly, these phenotypes were first discovered in or since have been verified in higher-organism models of synucleinopathies. Additionally, studies in yeast established a previously unknown link between α-syn and a second parkinsonism-associated protein, ATP13A2, and also connected both of these proteins to manganese homeostasis (19). Finally, high-throughput yeast screens have identified compounds that rescue both yeast and neuronal cells from α-syn–induced toxicity. These same compounds rescue neuronal models from mitochondrial poisons associated with PD (18). Thus, we and others have taken advantage of the high conservation of eukaryotic cell biology and the ease of genetic manipulation in yeast cells to provide insights into α-syn function and toxicity that are directly relevant to neuropathology.

Here we use a yeast model to investigate naturally occurring splice isoforms of α-syn. Full-length α-syn (α-synFL) contains seven exons (20). [Note: Exon numbering has been adjusted recently, because of the discovery of a new exon (21).] Exons one and two, and part of exon three, constitute the 5′ UTR of the mRNA. The remainder of exon three, exon four, and part of exon five comprise the N-terminal region of the protein; the rest of exon five and exons six and seven create the C-terminal tail of the protein. Both exon four and exon six are subject to alternative splicing, creating α-synΔ4 and α-synΔ6, respectively. These variants are differentially expressed in various synucleinopathies (20, 21), and recent work has tied PD risk factors to increased splicing of exon six (22, 23). However, it is not clear whether this change in splicing contributes to pathology, is part of a protective mechanism, or is functionally inconsequential.

To determine the significance of splice isoform changes, we compared the biological effects of α-synΔ4, α-synΔ6, and α-synFL. We characterized differences in the localization of each isoform and their relative toxicities. We tested the effects of 77 genes previously shown to modify the toxicity of α-synFL against the splice isoforms (17) and uncovered a differential response to the oxysterol-binding protein homolog 3 (Osh3p). This result, in turn, led us to study the sensitivity of cells expressing α-syn and its isoforms to perturbations in sterol synthesis.

Results

Splice Isoforms of α-Syn Display Different Toxicity. To investigate how variations in splicing affect the toxicity of α-syn, we created strains that expressed equal copies of α-synFL, α-synΔ4, or α-synΔ6 (Fig. 1*A*). Genes encoding these variants were integrated into the *HIS3*, *LEU2*, *TRP1*, and *URA3* loci. Such transformants can contain multiple tandem integrants per locus, potentially confounding their comparison. Therefore, we designed a PCR-based method to detect single integrants (Fig. S1) and generated strains containing single integrations of all isoforms at each locus (Fig. 1*B*). Using these single-integrant strains allowed a precisely controlled comparison. All the genes were driven by the same galactose-inducible promoter, so expression could be induced simply by shifting cells to galactose-containing medium. As expected, increasing copy number increased expression of the RNAs. (However, because of limiting concentrations of regulatory factors for galactose induction, mRNA levels did not increase linearly with more than three copies of the gene; Fig. 1*C*). See Table S1 for a complete list of strains used in this study.

Each protein variant accumulated to approximately the same level after galactose induction, indicating that the proteins have similar turnover rates (Fig. 1*D*). As expected, strains carrying four copies of α-synFL (4× α-synFL) displayed strong toxicity. In contrast, 4× α-synΔ6 strains showed only marginal toxicity, and 4× α-synΔ4 strains grew as well as the GFP control strain (Fig. 2*A*). Thus, when individually expressed, the proteins produced by the splice variants have very different inherent toxicities.

In the brain, the splice isoforms presumably are expressed in cells that also express α-synFL. To assess the ability of these

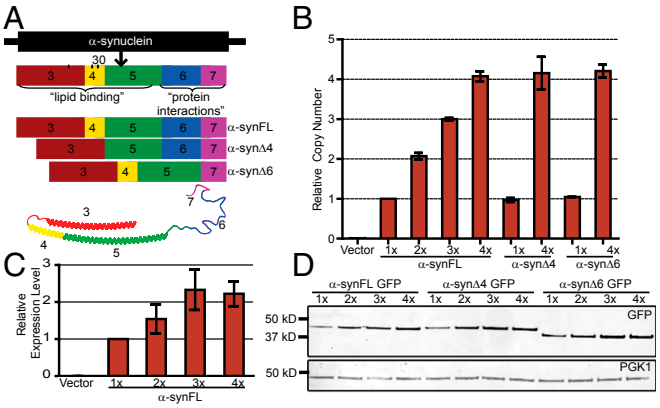

Fig. 1. Creation of strains with equal gene copy numbers of α-syn splice isoforms. (*A*) Summary of isoforms tested. Exons are indicated by number and color. A schematic of the helical structure of the portion of the protein encoded by exons 3, 4, and 5 and the unstructured portion encoded by exons 6 and 7 is shown. (*B*) Real-time PCR analysis of DNA levels of splice isoform strains expressing different gene copy numbers of α-syn, compared with a strain expressing one copy of α-synFL. 1×–4× represent the α-syn copy numbers. $n = 2$; error bars indicate SD. (*C*) Real-time PCR analysis of RNA levels upon induction of α-synFL strains, compared with a strain expressing one copy of α-synFL. 1×–4× represent the α-syn copy numbers. $n = 3$; error bars indicate SD. (*D*) Western blot of strains with 1×–4× copies of α-syn splice isoforms. 3-phosphoglycerate kinase (PGK1) served as the loading control.

isoforms to contribute to the toxicity of α-synFL, we constructed strains with two copies (2×) of each splice isoform and two copies of α-synFL. Strains expressing only 2× α-synFL showed little growth defect, in keeping with the dosage sensitivity previously reported for this protein (5). With this 2× level of α-synFL, however, the addition of two copies of either splice isoform was toxic. α-SynΔ4 enhanced toxicity to a lesser degree than α-synΔ6 (Fig. 2*B*). Therefore, although both splice isoforms are intrinsically less toxic than the WT protein, they can contribute to the toxicity of the full-length protein. To investigate how these isoforms differentially perturb the biology of the cell, we continued the remainder of our investigations on the

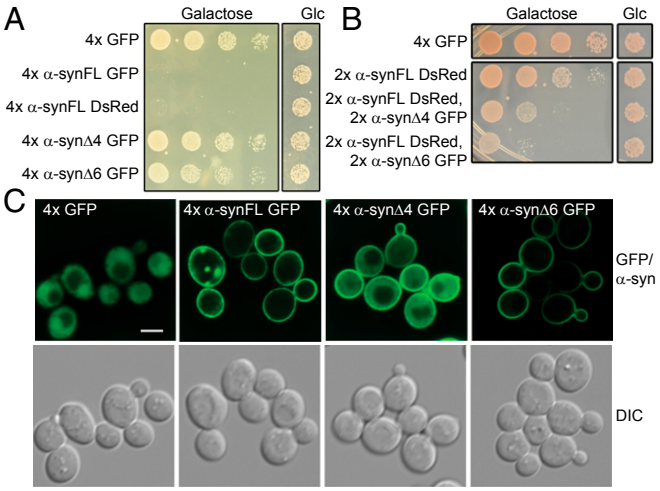

Fig. 2. α-Syn splice isoforms elicit different toxicities and localization when expressed at the same level. (*A*) Spot assay of α-syn–expressing strains with four copies of the indicated isoforms. Glc, glucose. (*B*) Spot assay of strains coexpressing two copies of α-synFL and two copies of the splice isoforms. Glc, glucose. (*C*) Fluorescent microscopy reveals differential localization of α-syn splice isoforms. (Scale bar, 5 μm.)

CELL BIOLOGY

isoforms expressed in isolation, starting by examining their localization patterns.

Splice Isoforms of α-Syn Display Different Localization. As previously reported, when first induced, α-synFL localizes to the plasma membrane (5). As it accumulates to toxic levels, it begins to form foci, first around the periphery of the cell and then extending into the interior (24). In the 4× strains, after 6 h of induction, α-synFL was observed at the plasma membrane as well as in foci (Fig. 2*C*). α-SynΔ4 lacks a portion of the N-terminal amphipathic helix required for lipid binding and localized to the plasma membrane less efficiently. α-SynΔ6, which has an intact lipid-binding domain, was localized primarily to the plasma membrane (Fig. 2*C*). At this level of expression, α-synΔ4 and α-synΔ6 rarely formed foci. These results confirm the previously reported role of the N-terminal lipid-binding domain in foci formation (25) and also implicate the C-terminal protein–protein interaction domain in this process. That α-synFL foci are the sites of accumulation of blocked vesicles (24) and both splice isoforms display reduced foci suggests both domains are involved in controlling vesicular trafficking.

Expression of α-Syn Splice Isoforms Blocks Vesicular Trafficking. We previously have described several cellular processes that are affected by α-syn in yeast and have determined the effect of most genes in the genome on α-syn toxicity (5, 17). Taking full advantage of yeast genetics to investigate functional distinctions between splice isoforms required the comparison of strains with similar levels of toxicity (Fig. 3*A*). To create them, we isolated transformants with different numbers of tandem integrations, selecting those with similar levels of toxicity, irrespective of copy number (Fig. 3 *B* and *C*). In these strains, α-synFL showed the expected localization pattern, forming small foci around the perimeter of the cells and larger foci in the cytoplasm (Fig. 3*D*). α-SynΔ4 and α-synΔ6 also formed foci, but α-synΔ4 still showed high levels of cytoplasmic localization.

One of the earliest toxicities associated with α-syn expression is a block in vesicle trafficking (17). To assess whether all splice isoforms could inhibit secretion, we used a halo assay for mating factor secretion. Cells of one mating type are spotted onto a lawn of the other mating factor type, and halos of growth arrest provide a qualitative measure of mating factor secretion. In tests on glucose plates, no α-syn was expressed, and halos were roughly equal in size. In contrast, when spotted on inducing galactose plates, strains expressing similarly toxic levels of all three α-syn splice isoforms showed similarly reduced zones of inhibition. This result suggested that all three variants are capable of inhibiting secretion (Fig. 4*A*). Importantly, this phenotype was not a generic effect of expressing a toxic protein; toxic levels of the Alzheimer's disease-related peptide Aβ (26) had little effect on trafficking.

We next asked if the foci formed by the splice isoforms involved clusters of vesicles that were blocked from fusing with their target membrane, as in the case of α-synFL (24). This phenotype can be probed by assaying colocalization of α-syn and vesicle-pathway proteins (24). Although trafficking of ER-to-Golgi secretory vesicles may be more sensitive to α-syn, we used the endocytic vesicle marker vacuolar protein sorting 21 (Vps21p) for this analysis, because it has been shown previously that overexpression of *VPS21* does not perturb α-syn localization (17, 24). Indeed, colocalization was observed between Vps21p and α-synFL as well as between Vps21p and α-synΔ4 and between Vps21p and α-synΔ6 (Fig. 4*B*). In contrast, clatherin heavy-chain protein Chc1p, which also associates with endocytic vesicles but disassembles immediately after vesicles form, did not colocalize with any of the variants (Fig. S2*A*). This result suggested that α-synFL and both splice isoforms of α-syn cause an accumulation of stalled trafficking vesicles.

α-Syn Splice Isoforms Show Differential Responses to OSH3 Overexpression. To investigate more thoroughly the mechanisms by which the splice isoforms induce toxicity, we tested all 77

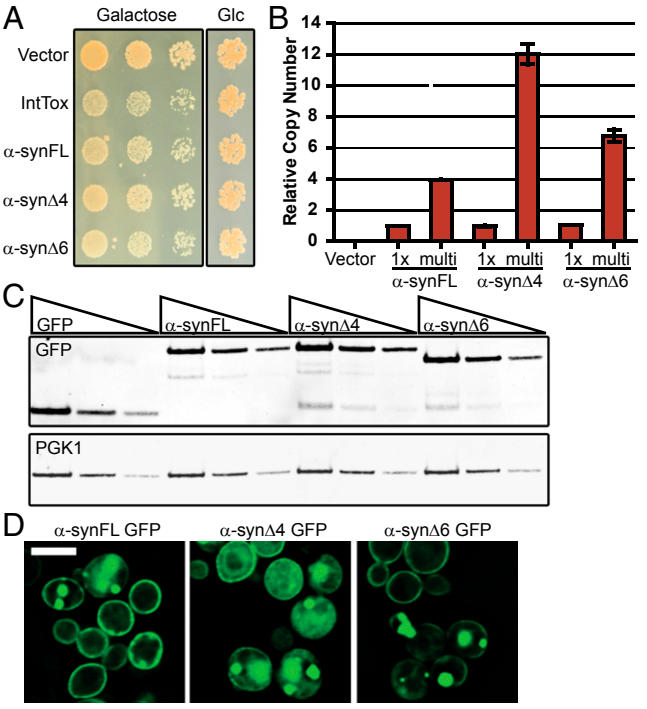

Fig. 3. Higher levels of α-syn splice isoform expression lead to higher toxicity and foci formation. (*A*) Spot assay of α-syn–expressing strains with different numbers of gene copies but equal levels of toxicity. IntTox is a previously created strain expressing α-synFL-YFP that was used in a high-throughput overexpression screen. Glc, glucose. (*B*) Quantification by real-time PCR of the number of α-syn copies inserted into the multicopy strains, compared with the 1× α-synFL strain. $n = 2$; error bars indicate SD. (*C*) Western blot analysis of α-syn splice isoforms in the multicopy strains shown in *A*. PGK1 served as loading control. (*D*) Fluorescence microscopy of the multicopy strains shown in *A*. (Scale bar, 5 μm.)

genes that previously had been identified as suppressors or enhancers of α-synFL–induced toxicity (17, 27). Each gene was tested at least three times against each splice isoform strain and against the full-length protein (Fig. S3).

Strikingly, most of the genes tested affected each of the splice isoforms in the same direction and to the same extent as α-synFL (Fig. 4*C* and Table S2). In congruence with the above results, all the vesicle trafficking-related modifiers affected α-synFL, α-synΔ4, and α-synΔ6 similarly. However, a small number of genes modified the toxicity of the two splice variants in a manner distinct from their effect on α-synFL. These effects were confirmed in individual spotting assays. Pho80p, a cyclin that monitors stress caused by nutrient starvation, enhances α-synΔ6 toxicity while suppressing α-synFL and α-synΔ4 toxicity. Furthermore, Osh3p suppressed toxicity of the α-synFL–expressing strain but enhanced toxicity of α-synΔ4 and α-synΔ6.

Osh3p belongs to a family of oxysterol-binding proteins; yeast cells have seven OSH homologs (28). Previous work showed that oxysterol-binding protein homolog 2 (OSH2) overexpression also could rescue α-synFL (17). Therefore, we were interested in assessing how overexpression of the other OSH family members affects strains expressing α-syn splice isoforms. Although it did not elicit as strong a phenotype when tested in high throughput, Osh2p did enhance α-synΔ4– and α-synΔ6–induced toxicity in this more thorough, low-throughput assay (Fig. S4). None of the other OSH family members affect α-syn–induced toxicity.

α-SynFL and α-SynΔ6, but not α-SynΔ4, Elicit Sensitivity to Simvastatin and Fluconazole. Given the role of Osh2p and Osh3p in mediating cellular sterol localization (29) and recent, somewhat perplexing, connections between PD and cholesterol in

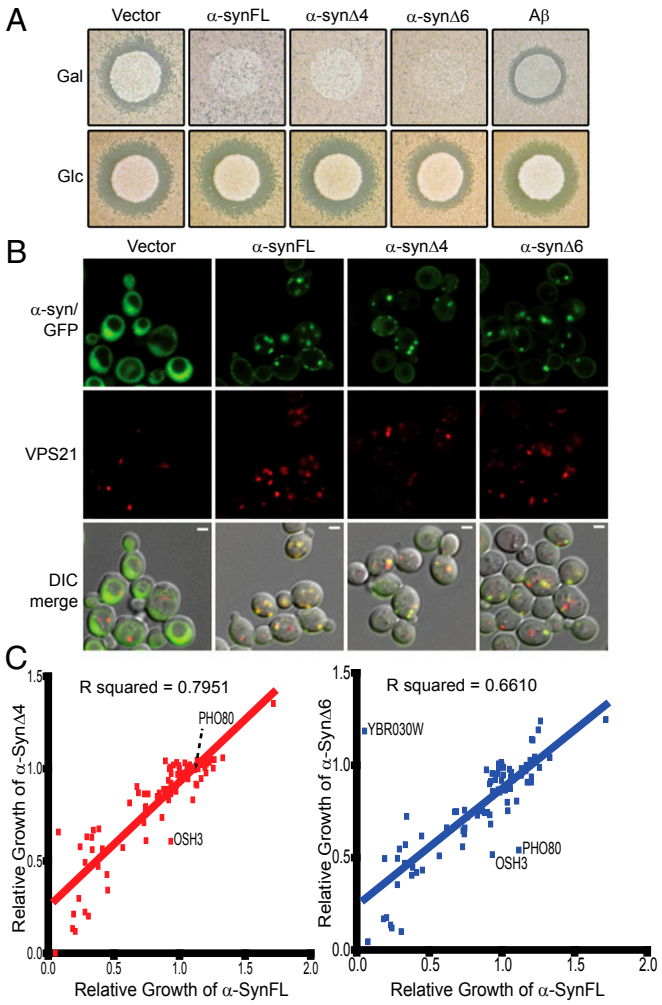

Fig. 4. Splice isoforms elicit toxicity by similar, but not identical, mechanisms. (*A*) Halo assays to test secretion capacities of α-syn–expressing cells. Mating type α cells were spotted on a lawn of *bar1* mating type α cells. Aβ, control; Gal, galactose; Glc, glucose. (*B*) Fluorescent microscopy of cells expressing α-syn isoforms tagged with GFP and mKate-Vps21p. In the bottom row, the DIC image is merged with both fluorescent images to show overlap of signal. (Scale bars, 2 μm.) (*C*) Relative growth of α-synFL–expressing strains transformed with genetic modifiers of toxicity compared with α-synΔ4– (red) or α-synΔ6– (blue) expressing strains. Each point represents the growth of the strain transformed with one genetic modifier. All hits shown were repeated upon retesting, with the exception of YBR030W. The effects of PHO80 were repeated in low throughput but are not considered further in this work.

human patients (30–32), we focused on the relationship between sterols and α-syn toxicity. *S. cerevisiae* cells use ergosterol, rather than cholesterol, as their principle sterol, but the two molecules are very similar and serve the same function in maintaining correct fluidity of the plasma membrane. α-SynFL–expressing yeast cells were sensitive to treatment with statins, which inhibit the protein that catalyzes a rate-limiting step in the production of sterols (27). Therefore, we asked whether cells expressing the splice isoforms of α-syn were similarly sensitive to treatment with simvastatin, a statin commonly prescribed in humans.

The sensitivity of yeast cells to simvastatin was increased by α-synFL and α-synΔ6 but not by α-synΔ4 (Fig. 5*A*). Statins inhibit a very early step in sterol production and disrupt multiple pathways related to α-syn–induced phenotypes, such as the production of quinones, dolichol formation, and prenylation. To focus more precisely on sterol metabolism, we took advantage of the more specific inhibitor fluconazole, which inhibits a downstream enzyme specific to ergosterol synthesis. Yeast treated with fluconazole accumulate a modified sterol, 14α-methyl-3, 6-diol, which increases membrane fluidity (33). We treated yeast expressing α-syn splice isoforms with concentrations of fluconazole that were not toxic to control cells. Again, α-synFL and

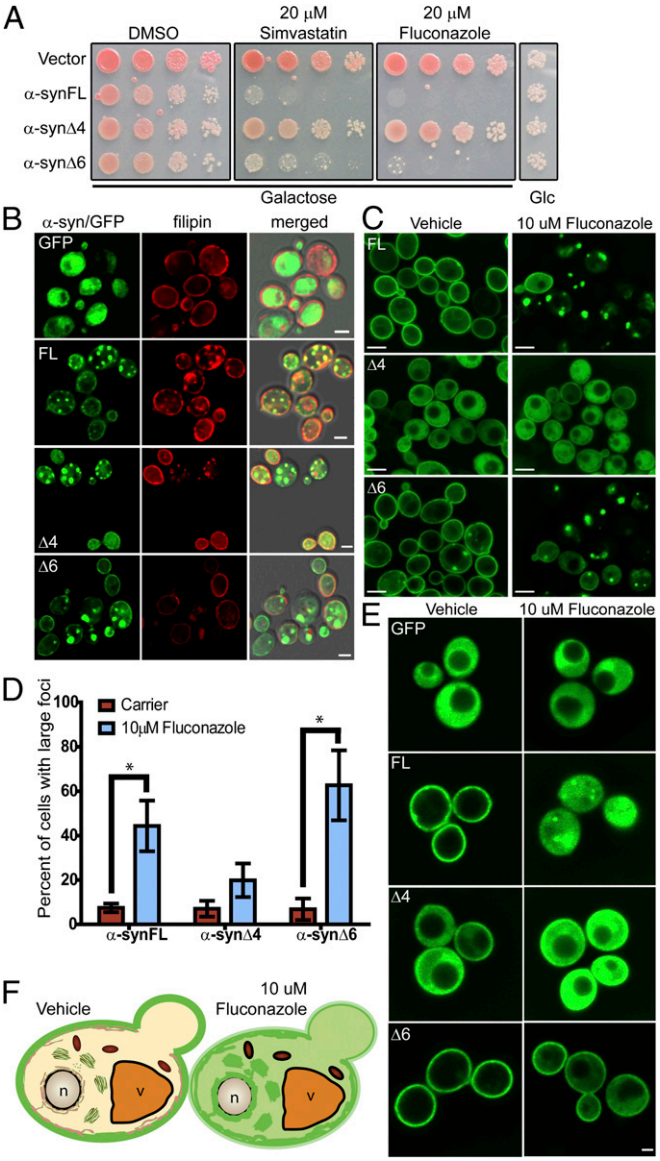

Fig. 5. α-Syn splice isoforms show differential sensitivity to changes in ergosterol levels. (*A*) Spot assay comparing the sensitivities of strains expressing α-syn splice isoforms to simvastatin and fluconazole. Glc, glucose. (*B*) Fluorescent microscopy showing partial colocalization of α-syn-GFP (green) and ergosterol (filipin, red). FL, α-synFL; Δ4, α-synΔ4; Δ6, α-synΔ6. (Scale bars 2 μm.) (*C*) Fluorescence microscopy showing the impact of fluconazole treatment on α-syn foci formation. (Scale bars, 5 μm.) (*D*) Percentage of cells with α-syn foci after 4 h of induction in the presence and absence of fluconazole. $n = 3$; error bars indicate SD; $^*P < 0.05$. (*E*) Fluorescence microscopy showing the impact of fluconazole treatment on α-syn localization. Cells lacking foci were chosen to highlight membrane binding. (Scale bar, 2 μm.) (*F*) Model of the proposed mechanism by which fluconazole enhances α-synFL and α-synΔ6 toxicity. Green indicates the localization of α-syn, which normally interacts with the plasma membrane and components of the secretory pathway, including the ER, Golgi, and vesicles. Upon fluconazole treatment, less α-syn associates with the plasma membrane, so more α-syn is cytoplasmic and interacts with the secretory pathway. n, nucleus; v, vacuole.

α-synΔ6 were sensitive to fluconazole treatment, whereas cells expressing α-synΔ4 were not affected (Fig. 5*A*). Therefore, a shift in sterol balance and an increase in membrane fluidity sensitize cells to α-synFL and α-synΔ6, but α-synΔ4 resists this effect.

α-Syn–Induced Sensitivity to Fluconazole Can Be Attributed to an Increased Trafficking Block. Because α-synFL foci represent lipid-rich, vesicular clusters blocked in trafficking by α-synFL, we investigated whether these clusters were enriched in sterols by staining with filipin, a fluorescent probe that binds sterols (34). In control cells, filipin displayed canonical staining of the plasma membrane, which has the highest sterol content in the cell (Fig. 5*B*) (35). In strains expressing α-synFL or either of the two isoforms of α-syn, filipin colocalized both to the plasma membrane and to large intracellular α-syn foci (Fig. 5*B*). Intriguingly, in many cases, some foci stained with filipin, but others did not. This observation suggests heterogeneity in the membrane sterol content of vesicles trapped at these foci.

Most notably, in cells that had higher concentrations of filipin at α-syn foci, there was less filipin staining at the plasma membrane. Therefore, expression of α-syn leads to a redistribution of endogenous sterols. It is possible that this redistribution results from the impact of α-syn on vesicular trafficking, because one mechanism by which sterols arrive at the plasma membrane is by transport through the secretory pathway (29). Because α-syn expression blocks vesicular trafficking, sterol transport also may be impeded by α-syn expression.

How might fluconazole treatment affect α-syn localization? Incubation with fluconazole elicited a striking relocalization of α-synFL and of α-synΔ6 but not of α-synΔ4 (Fig. 5*C*). α-SynFL– and α-synΔ6–expressing cells treated with fluconazole were much more likely to form foci, even at a time point when untreated cells show few foci (Fig. 5*D*). These foci colocalized with Vps21p (Fig. S2*B*). Together with previous work, this result indicates that they are composed of α-syn decorating clumps of stalled trafficking vesicles (24). When cells without significant foci were examined, it also was clear that some of the α-synFL and α-synΔ6 protein redistributed to the cytoplasm (Fig. 5*E*). This observation suggests that reductions in plasma membrane sterols reduce binding of α-synFL and α-synΔ6 to that membrane. This reduction might be caused by a specific failure of α-syn to bind 14α-methyl-3,6-diol or, more broadly, by the impact of fluconazole on membrane fluidity (33). α-SynΔ4 bound membranes more weakly and did not respond to fluconazole treatment, suggesting that removal of exon four changes the ability of α-syn to interact with membranes, possibly mediated by changes in sterol binding.

Discussion

We have found that different splice isoforms of α-syn exhibit very different toxicities and membrane-binding properties in vivo. When expression levels of these proteins are adjusted to produce an equal level of toxicity, all isoforms derange cellular homeostasis by similar means, but there are differences in their response to perturbations in sterol homeostasis by the oxysterol-binding protein Osh3p. These differences led us to investigate how changes in the sterol content of cellular membranes might affect α-syn toxicity. We found that simvastatin and fluconazole reduced α-syn's interactions with the plasma membrane, increased its interactions with intracellular vesicles, and increased its toxicity.

Our work was enabled by the genetic toolbox available for yeast. Such investigations are much more difficult in neurons. However, because many features of eukaryotic cell biology and vesicle trafficking are conserved from yeast to neurons (14), as are many other aspects of α-syn toxicity (11), our findings are likely relevant to the cells of higher organisms. Importantly, the plasma membranes of yeast have the highest ratio of sterols to phospholipids of all membranes within the cells (35), and human cells have this same distribution (36). Indeed, neurons are sensitive to perturbations in cholesterol levels, with lowered cholesterol levels decreasing the rate of synaptic vesicle fusion (37).

In neurons α-syn is associated with secretory vesicles at the synapse. In yeast α-syn is found at the plasma membrane because the trafficking of secretory vesicles is constitutive in this organism. α-Syn does not seem to be toxic when localized to the plasma membrane. Rather, its toxicity derives from its impeding various steps in vesicle trafficking (15, 17, 24). Consequently, when α-syn is expressed at nontoxic levels, the plasma membrane—and presumably the synaptic vesicles of neurons, which also have a high sterol content (38)—might serve as a reservoir for the protein and thereby would reduce potentially toxic interactions of α-synFL and α-synΔ6 with vesicles associated with other stages of trafficking. Depletion of sterols from the plasma membrane would afford a greater opportunity for α-syn to interact in a toxic manner with earlier vesicles in the secretory and endocytic pathways (Fig. 5*F*).

There are other potential mechanisms for the data we present here. It is possible that, by disrupting trafficking, α-syn alters membrane fluidity, which in turn could affect sterol biosynthesis. Although yeast lacks an ortholog for SREPB, the main sterol-regulating transcription factor used in higher organisms, yeast do have two transcription factors, Upc2p and Ecm22p, which can perform similar functions (39, 40). Other parts of the pathway also are conserved (41). The presence of these pathways in yeast suggests that any perturbations to membrane homeostasis in yeast could have a large impact on the cell, complicating the interpretation of our results.

A remaining puzzle is that the response of both α-synΔ4 and α-synΔ6 to Osh3p overexpression was different from that of α-synFL, but a differential response to pharmacological sterol depletion was seen only with α-synΔ4. Osh3p belongs to a large family of oxysterol-binding proteins conserved from yeast to mammals. These proteins have partially overlapping functions in membrane sterol relocalization that have yet to be broadly elucidated. Recent work implicates Osh3p in regulating lipid concentrations at ER/plasma membrane contact sites (42). It is tempting to speculate that α-syn blocks transport between the ER and plasma membrane and that reorganization of sterols by OSH proteins affects the binding or functionality of α-syn. This change in membrane architecture may allow the splice isoforms to interact with the membrane and impart toxicity differently. Alternatively, Osh3p interacts with the RNA helicase, Rok1p, and has been shown to affect nuclear fusion upon overexpression (43). It is possible that Osh3p differentially affects α-syn–induced toxicity by interfacing with this pathway, and this possibility warrants further investigation. We suggest that α-syn and its two splice isoforms—which differentially affect protein::lipid interactions versus protein::protein interactions—will provide useful tools for disentangling the still poorly understood specificities of OSH protein function.

Currently there is considerable confusion about the relationship between cholesterol and synucleinopathies (30–32). Although some studies suggest that cholesterol-lowering drugs have a protective role, others point to associations between low cholesterol and increased risk of PD. Therefore, it is not yet clear how cholesterol levels affect PD occurrence and progression. Statins are one of the most heavily prescribed drugs in the developed world. However, we do not understand how these drugs and, more broadly, how other changes in sterol metabolism, affect the progression of synucleinopathies. Our work indicates that investigations of the effects of sterols and of α-syn splice isoforms in neurons and mouse models are warranted and, indeed, much needed.

Materials and Methods

Yeast Strains and Growth Conditions. Details concerning construction of strains and plasmids and growth conditions are given in *SI Materials and Methods*.

Real-Time PCR. Genomic DNA was extracted using the YeaStar Genomic DNA Kit (Zymoresearch) and RNA was extracted using an RNeasy Mini Kit (Qiagen) and converted to cDNA with a QuantiTect Reverse Transcription Kit (Qiagen).

Levels of α-syn and Pgk1p (control) then were measured using a QuantiFast SYBR Green PCR Kit (Qiagen) in triplicate.

Fluorescent Microscopy. Further details on fluorescent microscopy and image processing are given in *SI Materials and Methods*.

For localization studies in the presence of fluconazole, cells were induced as described in *SI Materials and Methods*. To examine localization changes in the presence of 10 μM fluconazole, the drug was added during growth in raffinose, and cells were treated overnight before being induced with galactose for 4 h. DMSO was used as the vehicle. After 4 h, cells were imaged as outlined in *SI Materials and Methods*, and foci were counted from GFP pictures taken of fields chosen in the differential interference contrast (DIC) channel to allow unbiased field selection. Weak interactions between GFP molecules can influence the localization of proteins to which they are fused. Hence we make no quantitative measurements of localization. Rather we compare only the relative changes in localization of different α-syn variants fused in an identical way to the same GFP construct, which did not associate with membranes on its own.

For filipin staining, cells were induced as described in *SI Materials and Methods*. After washing, they were resuspended in 4% (vol/vol) formaldehyde [diluted from 16% (wt/vol) formaldehyde (Ted Pella) in PBS] and were incubated for 15 min. After two washings in PBS, cells were stained with 500 μg/mL filipin (Cayman Chemical) for 10 min in the dark before visualization. Similar results were obtained with unfixed cells.

Spotting Assays. Cells were grown overnight to saturation in synthetic medium containing raffinose. Every strain was diluted to a starting $OD_{600} = 1.0$, and fivefold serial dilutions were made before spotting on inducing (galactose) or noninducing (glucose) plates.

Western Blots. After induction, cells were lysed by bead beating in lysis buffer [10 mM Hepes (pH 7.5), 10 mM NaCl, 1.5 mM $MgCl_2$, 20% (vol/vol) glycerol, 0.5 mM PMSF, and 1× protease inhibitor (Roche)]. Samples were run on a 10% Bis-Tris gel (Invitrogen). The proteins were transferred to PDVF membranes, which then were blocked with 5% (wt/vol) milk in 1× PBS. For protein visualization, either anti-GFP (Roche) or anti-PGK1 (Molecular Probes) was used as a primary antibody, and a dye-conjugated anti-mouse IgG (LICOR Biosciences) was used as a secondary antibody. The blots were visualized using the Odyssey Infrared Imaging System (LICOR Biosciences).

Secretion Assay. Strains were streaked onto a yeast extract/peptone (YP)-glucose plate and grown at 30 °C overnight. The next day, *bar1* cells were grown in YP-glucose for 4 h before being diluted to plate a lawn on both YP-glucose and YP-galactose plates. After drying, the test strains were resuspended in sterile water. For uninduced controls, 10 μL of culture diluted to an $OD_{600} = 1.0$ was spotted in the center of the YP-dextrose plate. For the cultures induced on YP-galactose plates, an $OD_{600} = 1.0$ was used for strains in the toxic disease model, and an $OD_{600} = 0.04$ was used for the vector control to account for their different rates of growth. Pictures were taken after 2 d of growth at 30 °C.

Statistics. All statistical analyses were performed using the Student's *t* test, with the exception of the goodness-of-fit analysis in which a linear regression was used to determine R^2.

ACKNOWLEDGMENTS. We thank members of the S.L. laboratory and Scott Valastyan for comments on this manuscript. The *bar1* cells were a kind gift of Gerald Fink. This work was funded by the Howard Hughes Medical Institute and the JPB Foundation. D.J.T. was funded by a National Research Service Awards fellowship. S.L. is an Investigator of the Howard Hughes Medical Institute.

1. Lee VM, Trojanowski JQ (2006) Mechanisms of Parkinson's disease linked to pathological alpha-synuclein: New targets for drug discovery. *Neuron* 52(1):33–38.
2. Polymeropoulos MH, et al. (1997) Mutation in the alpha-synuclein gene identified in families with Parkinson's disease. *Science* 276(5321):2045–2047.
3. Krüger R, et al. (1998) Ala30Pro mutation in the gene encoding alpha-synuclein in Parkinson's disease. *Nat Genet* 18(2):106–108.
4. Mizuta I, et al. (2006) Multiple candidate gene analysis identifies alpha-synuclein as a susceptibility gene for sporadic Parkinson's disease. *Hum Mol Genet* 15(7):1151–1158.
5. Outeiro TF, Lindquist S (2003) Yeast cells provide insight into alpha-synuclein biology and pathobiology. *Science* 302(5651):1772–1775.
6. Feany MB, Bender WW (2000) A Drosophila model of Parkinson's disease. *Nature* 404(6776):394–398.
7. Masliah E, et al. (2000) Dopaminergic loss and inclusion body formation in alpha-synuclein mice: Implications for neurodegenerative disorders. *Science* 287(5456):1265–1269.
8. Davidson WS, Jonas A, Clayton DF, George JM (1998) Stabilization of alpha-synuclein secondary structure upon binding to synthetic membranes. *J Biol Chem* 273(16):9443–9449.
9. Giasson BI, Murray IV, Trojanowski JQ, Lee VM (2001) A hydrophobic stretch of 12 amino acid residues in the middle of alpha-synuclein is essential for filament assembly. *J Biol Chem* 276(4):2380–2386.
10. Eliezer D, Kutluay E, Bussell R, Jr., Browne G (2001) Conformational properties of alpha-synuclein in its free and lipid-associated states. *J Mol Biol* 307(4):1061–1073.
11. Khurana V, Lindquist S (2010) Modelling neurodegeneration in Saccharomyces cerevisiae: Why cook with baker's yeast? *Nat Rev Neurosci* 11(6):436–449.
12. Thiam AR, et al. (2013) COPI buds 60-nm lipid droplets from reconstituted water-phospholipid-triacylglyceride interfaces, suggesting a tension clamp function. *Proc Natl Acad Sci USA* 110(33):13244–13249.
13. Pranke IM, et al. (2011) α-Synuclein and ALPS motifs are membrane curvature sensors whose contrasting chemistry mediates selective vesicle binding. *J Cell Biol* 194(1):89–103.
14. Wickner W, Schekman R (2008) Membrane fusion. *Nat Struct Mol Biol* 15(7):658–664.
15. Dixon C, Mathias N, Zweig RM, Davis DA, Gross DS (2005) Alpha-synuclein targets the plasma membrane via the secretory pathway and induces toxicity in yeast. *Genetics* 170(1):47–59.
16. Auluck PK, Caraveo G, Lindquist S (2010) α-Synuclein: Membrane interactions and toxicity in Parkinson's disease. *Annu Rev Cell Dev Biol* 26:211–233.
17. Cooper AA, et al. (2006) Alpha-synuclein blocks ER-Golgi traffic and Rab1 rescues neuron loss in Parkinson's models. *Science* 313(5785):324–328.
18. Su LJ, et al. (2010) Compounds from an unbiased chemical screen reverse both ER-to-Golgi trafficking defects and mitochondrial dysfunction in Parkinson's disease models. *Dis Model Mech* 3(3-4):194–208.
19. Gitler AD, et al. (2009) Alpha-synuclein is part of a diverse and highly conserved interaction network that includes PARK9 and manganese toxicity. *Nat Genet* 41(3):308–315.
20. Beyer K, Ariza A (2013) α-Synuclein posttranslational modification and alternative splicing as a trigger for neurodegeneration. *Mol Neurobiol* 47(2):509–524.
21. Beyer K, et al. (2008) Differential expression of alpha-synuclein, parkin, and synphilin-1 isoforms in Lewy body disease. *Neurogenetics* 9(3):163–172.
22. McCarthy JJ, et al. (2011) The effect of SNCA 3′ region on the levels of SNCA-112 splicing variant. *Neurogenetics* 12(1):59–64.
23. Kalivendi SV, Yedlapudi D, Hillard CJ, Kalyanaraman B (2010) Oxidants induce alternative splicing of alpha-synuclein: Implications for Parkinson's disease. *Free Radic Biol Med* 48(3):377–383.
24. Gitler AD, et al. (2008) The Parkinson's disease protein alpha-synuclein disrupts cellular Rab homeostasis. *Proc Natl Acad Sci USA* 105(1):145–150.
25. Volles MJ, Lansbury PT, Jr. (2007) Relationships between the sequence of alpha-synuclein and its membrane affinity, fibrillization propensity, and yeast toxicity. *J Mol Biol* 366(5):1510–1522.
26. Treusch S, et al. (2011) Functional links between Aβ toxicity, endocytic trafficking, and Alzheimer's disease risk factors in yeast. *Science* 334(6060):1241–1245.
27. Yeger-Lotem E, et al. (2009) Bridging high-throughput genetic and transcriptional data reveals cellular responses to alpha-synuclein toxicity. *Nat Genet* 41(3):316–323.
28. Beh CT, McMaster CR, Kozminski KG, Menon AK (2012) A detour for yeast oxysterol binding proteins. *J Biol Chem* 287(14):11481–11488.
29. Schulz TA, Prinz WA (2007) Sterol transport in yeast and the oxysterol binding protein homologue (OSH) family. *Biochim Biophys Acta* 1771(6):769–780.
30. Ghosh A, et al. (2009) Simvastatin inhibits the activation of p21ras and prevents the loss of dopaminergic neurons in a mouse model of Parkinson's disease. *J Neurosci* 29(43):13543–13556.
31. Huang XM, Abbott RD, Petrovitch H, Mailman RB, Ross GW (2008) Low LDL cholesterol and increased risk of Parkinson's disease: Prospective results from Honolulu-Asia Aging Study. *Mov Disord* 23(7):1013–1018.
32. Wolozin B, et al. (2007) Simvastatin is associated with a reduced incidence of dementia and Parkinson's disease. *BMC Med* 5:20.
33. Abe F, Usui K, Hiraki T (2009) Fluconazole modulates membrane rigidity, heterogeneity, and water penetration into the plasma membrane in Saccharomyces cerevisiae. *Biochemistry* 48(36):8494–8504.
34. Norman AW, Demel RA, de Kruyff B, Geurts van Kessel WS, van Deenen LL (1972) Studies on the biological properties of polyene antibiotics: Comparison of other polyenes with filipin in their ability to interact specifically with sterol. *Biochim Biophys Acta* 290(1):1–14.
35. Zinser E, et al. (1991) Phospholipid synthesis and lipid composition of subcellular membranes in the unicellular eukaryote Saccharomyces cerevisiae. *J Bacteriol* 173(6):2026–2034.
36. Maxfield FR, Menon AK (2006) Intracellular sterol transport and distribution. *Curr Opin Cell Biol* 18(4):379–385.
37. Linetti A, et al. (2010) Cholesterol reduction impairs exocytosis of synaptic vesicles. *J Cell Sci* 123(Pt 4):595–605.
38. Takamori S, et al. (2006) Molecular anatomy of a trafficking organelle. *Cell* 127(4):831–846.
39. Vik A, Rine J (2001) Upc2p and Ecm22p, dual regulators of sterol biosynthesis in Saccharomyces cerevisiae. *Mol Cell Biol* 21(19):6395–6405.
40. Marie C, Leyde S, White TC (2008) Cytoplasmic localization of sterol transcription factors Upc2p and Ecm22p in S. cerevisiae. *Fungal Genet Biol* 45(10):1430–1438.
41. Nielsen J (2009) Systems biology of lipid metabolism: From yeast to human. *FEBS Lett* 583(24):3905–3913.
42. Stefan CJ, et al. (2011) Osh proteins regulate phosphoinositide metabolism at ER-plasma membrane contact sites. *Cell* 144(3):389–401.
43. Park YU, Hwang O, Kim J (2002) Two-hybrid cloning and characterization of OSH3, a yeast oxysterol-binding protein homolog. *Biochem Biophys Res Commun* 293(2):733–740.

Supporting Information

Valastyan et al. 10.1073/pnas.1324209111

SI Materials and Methods

Materials. Simvastatin was obtained from Sigma-Aldrich. Fluconazole was obtained from VWR.

Yeast Strains and Growth Conditions. All experiments were performed in the W303 background unless otherwise noted. Secretion assays used a *bar1* mutant strain, which was a gift from the Fink laboratory (Whitehead Institute, Cambridge, MA). The standard lithium acetate transformation protocol was used for all transformations (1). To select for single integrants, ~50 ng of cut plasmid DNA was used in the transformation, resulting in a mix of single and tandem integrants. To select for tandem integrants, ~500 ng of cut plasmid DNA was used in the transformation. Although all data used fusions with fluorescent proteins, untagged α-synuclein (α-syn) splice isoforms were retested in multiple experiments and behaved similarly.

Standard conditions were used for all yeast growth. For galactose induction, unless otherwise noted, cells were grown to log phase for 6–8 h in synthetic medium containing glucose before being diluted into synthetic medium containing raffinose for overnight growth. Log-phase cells then were diluted into synthetic medium containing galactose for induction. Unless otherwise specified, cells were induced for 6 h.

For screening suppressors and enhancers, a standard lithium acetate transformation protocol was adapted for use with 96-well plates (1, 2). After 2 d of growth, galactose plates were scanned, and the density of the spot was analyzed using ImageQuant TL. This process was repeated at least three times for each strain.

Synthetic medium included 0.67% yeast nitrogen base without amino acids (Fischer Scientific) supplemented with amino acids as needed (MP Biomedicals) and 2% (wt/vol) sugar. Yeast extract/peptone medium included 1% yeast extract, 2% peptone, 2% glucose adjusted to pH 7.0, and 2% sugar. Plates included 2% agar.

Plasmid Construction. A seventh exon of α-syn was found recently. Therefore, in many previous works, α-synΔ4 is referred to as "α-syn lacking exon 3" or "α-syn126," and α-synΔ6 is referred to as "α-syn lacking exon 5" or "α-syn112" (3). α-Syn splice isoforms were generated using overlap-extension PCR with Pfu Turbo (Agilent Technologies). The second round of PCR also added the sequences required for subcloning via BP reaction into pDONR221 (Invitrogen) (4, 5). The resulting entry clone then was used in an LR reaction to move the insert to a variety of necessary entry vectors, all from the pAG series (6).

For screening previously established genetic modifiers of α-syn–induced toxicity, the hits were cherry-picked from the Yeast FLEXGene collection (7). Any gene used in low throughput was cherry-picked from the original library and sequence-verified. If required in a different backbone, the gene was moved to pDONR221 by BP reaction and then to a vector of the pAG series by LR reaction. mKate-*CHC1* and mKate-*VPS21* were inserted with the same protocol into pRS-GPD-mKate-ccdB.

Single-Insertion PCR Analysis. Colony PCR was used to screen all strains for those with a single insertion in the correct locus (Fig. S1*A*). Correct strains were those that PCR-amplified bands with primers A+B and C+D but not A+D and B+C. Those that were correct by this first screening were analyzed by long-extension PCR (Roche).

Microscopy Processing. Cells were induced following standard galactose induction before visualization by fluorescent microscopy. Cells were spun down, washed, and resuspended in 1× PBS before being viewed with a Plan Apochromat 100×/1.40 NA oil objective lens on a Nikon Eclipse Ti microscope at room temperature. Images were taken with a CoolSNAP HQ camera (Photometrics). Z stacks were taken above and below the plane of focus and then were deconvoluted by using the 3D deconvolution algorithm in the NIS-Elements HR software.

1. Gietz RD, Schiestl RH, Willems AR, Woods RA (1995) Studies on the transformation of intact yeast cells by the LiAc/SS-DNA/PEG procedure. *Yeast* 11:355–360.
2. Cooper AA, et al. (2006) Alpha-synuclein blocks ER-golgi traffic and Rab1 rescues neuron loss in Parkinson's models. *Science* 313(5785):324–328.
3. Beyer K, Ariza A (2013) α-Synuclein posttranslational modification and alternative splicing as a trigger for neurodegeneration. *Mol Neurobiol* 47(2):509–524.
4. Hartley JL, Temple GF, Brasch MA (2000) DNA cloning using in vitro site-specific recombination. *Genome Res* 10:1788–1795.
5. Walhout AJ, et al. (2000) GATEWAY recombinational cloning: application to the cloning of large numbers of open reading frames or ORFeomes. *Methods Enzymol* 328:575–592.
6. Alberti S, Gitler AD, Lindquist S (2007) A suite of Gateway cloning vectors for high-throughput genetic analysis in *Saccharomyces cerevisiae*. *Yeast* 24(10):913–919.
7. Hu Y, et al. (2007) Approaching a complete repository of sequence-verified protein-encoding clones for *Saccharomyces cerevisiae*. *Genome Res* 17:536–543.

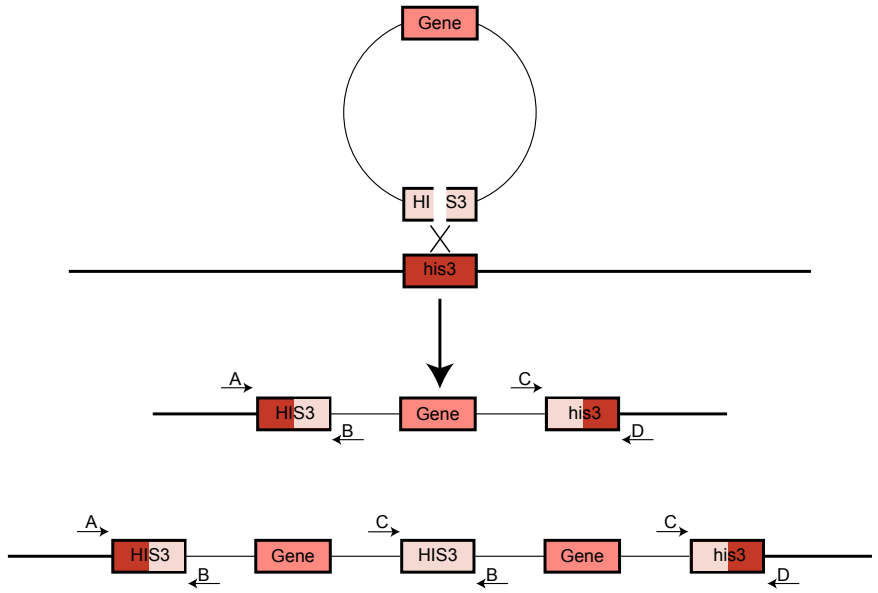

Fig. S1. Diagram showing the primer placement for testing for single integration of pRS plasmids. Primers were designed to be used regardless of the identity of the inserted gene. Colony PCR was used with primer sets A+B, C+D, A+D, and B+C. A+B and C+D would result in a band if there was a correct insertion; A+D would result in a band if there was no correct insertion, and B+C would result in a band if there were tandem insertions. After this screening, long-extension PCR was used with primers A+D to confirm the results.

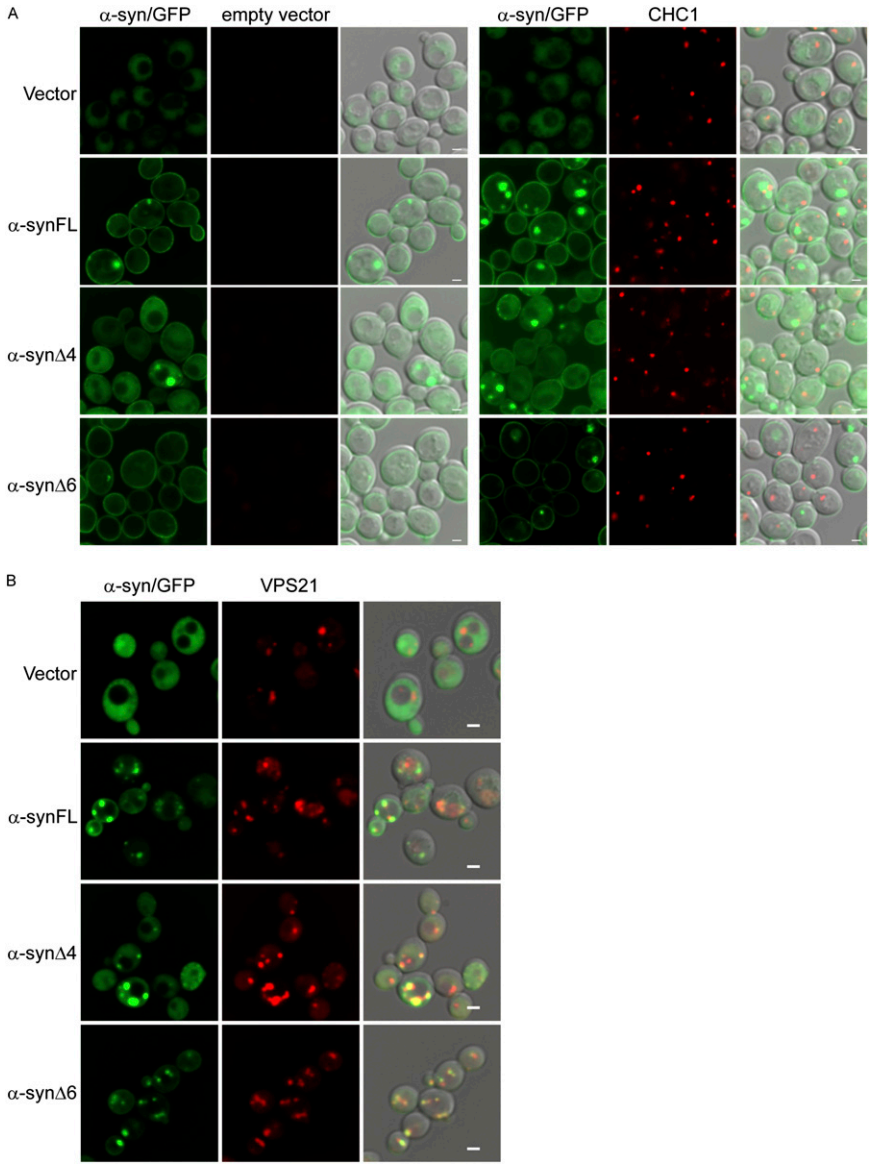

Fig. S2. (*A*) Fluorescent microscopy of α-syn-GFP–expressing cells with the addition of an empty vector or mKate-clathrin heavy chain 1 (Chc1p). (Scale bars, 2 μm.) (*B*) Fluorescent microscopy showing colocalization of α-syn-GFP and mKate-vacuolar protein sorting 21 (Vps21p). (Scale bars, 2 μm.)

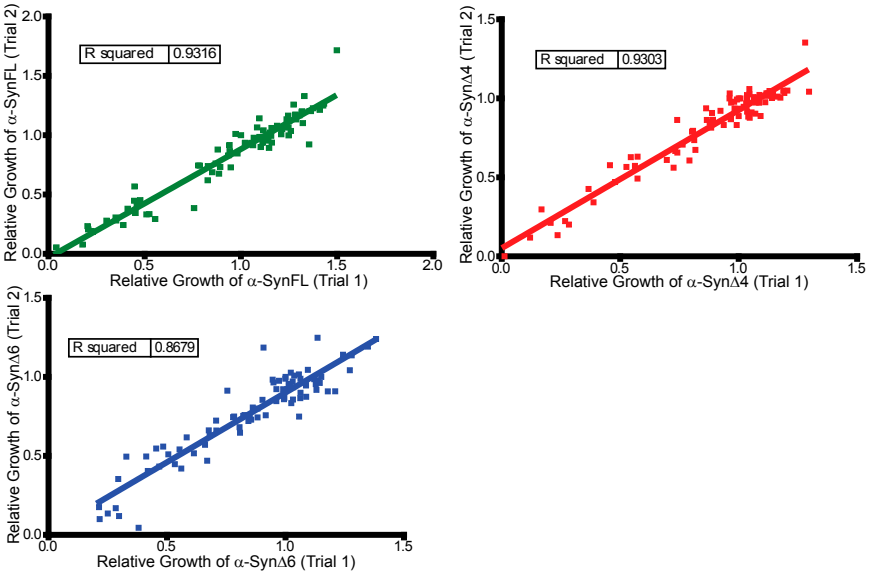

Fig. S3. High-throughput transformation of splice isoforms with genetic modifiers of α-syn–induced toxicity produced reproducible results. Each spot on each graph represents the rate of growth of one splice isoform of α-syn strain transformed with one genetic modifier on two separate trials.

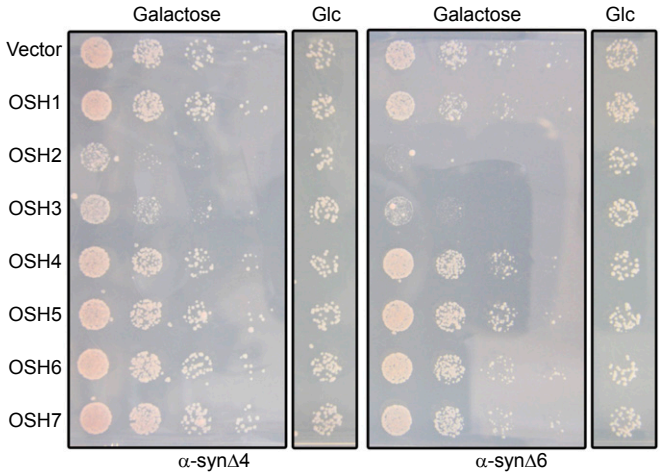

Fig. S4. Spot test analysis of the α-syn splice isoform–expressing strains in the presence of all seven OSH family members. Glc, glucose.

Table S1. Strain list

Strain	Genotype
1× α-synFL GFP	W303 mat a pAG306 Gal α-synFL GFP
2× α-synFL GFP	W303 mat a pAG305 Gal α-synFL GFP pAG306 Gal α-synFL GFP
3× α-synFL GFP	W303 mat a pAG304 Gal α-synFL GFP pAG305 Gal α-synFL GFP pAG306 Gal α-synFL GFP
4× α-synFL GFP	W303 mat a pAG303 Gal α-synFL GFP pAG304 Gal α-synFL GFP pAG305 Gal α-synFL GFP pAG306 Gal α-synFL GFP
4× α-synFL DsRed	W303 mat a pAG303 Gal α-synFL DsRed pAG304 Gal α-synFL DsRed pAG305 Gal α-synFL DsRed pAG306 Gal α-synFL DsRed
1× α-synΔ4 GFP	W303 mat a pAG306 Gal α-synΔ4 GFP
4× α-synΔ4 GFP	W303 mat a pAG303 Gal α-synΔ4 GFP pAG304 Gal α-synΔ4 GFP pAG305 Gal α-synΔ4 GFP pAG306 Gal α-synΔ4 GFP
1× α-synΔ6 GFP	W303 mat a pAG306 Gal α-synΔ6 GFP
4× α-synΔ6 GFP	W303 mat a pAG303 Gal α-synΔ6 GFP pAG304 Gal α-synΔ6 GFP pAG305 Gal α-synΔ6 GFP pAG306 Gal α-synΔ6 GFP
2× α-synFL DsRed	W303 mat a pAG303 Gal α-synΔ4 GFP pAG304 Gal α-synFL
2× α-synΔ4 GFP	DsRed pAG305 Gal α-synFL DsRed pAG306 Gal α-synΔ4 GFP
2× α-synFL DsRed	W303 mat a pAG303 Gal α-synΔ6 GFP pAG304 Gal α-synFL
2× α-synΔ6 GFP	DsRed pAG305 Gal α-synFL DsRed pAG306 Gal α-synΔ6 GFP
Vector a	W303 mat a pAG303 Gal GFP pAG304 Gal GFP
α-synFL multicopy a	W303 mat a pAG303 Gal α-synFL GFP pAG304 Gal α-synFL GFP
α-synΔ4 multicopy a	W303 mat a pAG303 Gal α-synΔ4 GFP pAG304 Gal α-synΔ4 GFP
α-synΔ6 multicopy a	W303 mat a pAG303 Gal α-synΔ6 GFP pAG304 Gal α-synΔ6 GFP
Vector α	W303 mat α pAG303 Gal GFP pAG304 Gal GFP
α-synFL multicopy α	W303 mat α pAG303 Gal α-synFL GFP pAG304 Gal α-synFL GFP
α-synΔ4 multicopy α	W303 mat α pAG303 Gal α-synΔ4 GFP pAG304 Gal α-synΔ4 GFP
α-synΔ6 multicopy α	W303 mat α pAG303 Gal α-synΔ6 GFP pAG304 Gal α-synΔ6 GFP
Aβ	W303 mat α pAG305 Gal Aβ
bar1	mat a bar1 leu2 ura3 trp1 his2 ade1

Table S2. Genes tested in high-throughput analysis of α-syn suppressors and enhancers

Yeast gene	Effect with α-synFL	Effect with α-synΔ4	Effect with α-synΔ6
Amino acid transport			
AVT4	Suppressor	Suppressor	Suppressor
DIP5	Suppressor	Suppressor	Suppressor
LST8	Suppressor	Suppressor	Suppressor
Autophagy			
NVJ1	Suppressor	Suppressor	Suppressor
Cytoskeleton			
ICY1	Suppressor	Suppressor	Suppressor
ICY2	Suppressor	Suppressor	Suppressor
Manganese transport			
CCC1	Suppressor	Suppressor	Suppressor
PMR1	Enhancer	Enhancer	Enhancer
Protein phosphorylation			
IME2	Suppressor	Suppressor	Suppressor
PTP2	Suppressor	Suppressor	Suppressor
GIP2	Suppressor	Suppressor	Suppressor
YCK3	Suppressor	Suppressor	Suppressor
RCK1	Suppressor	Suppressor	Suppressor
CDC5	Suppressor	Suppressor	Suppressor
PTC4	Suppressor	Suppressor	Suppressor
SIT4	Enhancer	Enhancer	Enhancer
CAX4	Enhancer	Enhancer	Enhancer
PPZ2	Enhancer	Enhancer	Enhancer
PPZ1	Enhancer	Enhancer	Enhancer
Transcription/translation			
CUP9	Suppressor	Suppressor	Suppressor
HAP4	Suppressor	Suppressor	Suppressor
FZF1	Suppressor	Suppressor	Suppressor
MGA2	Suppressor	Suppressor	Suppressor
MKS1	Enhancer	Enhancer	Enhancer
VHR1	Suppressor	Suppressor	Suppressor
JSN1	Suppressor	Suppressor	Suppressor
SUT2	Enhancer	Enhancer	Enhancer
TIF4632	Suppressor	Suppressor	Suppressor
STB3	Suppressor	Suppressor	Suppressor
MATALPHA1	Enhancer	Less enhancement	Less enhancement
Trehalose biosynthesis			
UGP1	Suppressor	Suppressor	Suppressor
TPS3	Suppressor	Suppressor	Suppressor
NTH1	Suppressor	Suppressor	Suppressor
Ubiquitin-related			
CDC4	Suppressor	Suppressor	Suppressor
UIP5	Suppressor	Suppressor	Suppressor
HRD1	Suppressor	Suppressor	Suppressor
UBP11	Enhancer	Enhancer	Enhancer
UBP7	Enhancer	Enhancer	Enhancer
Vesicular transport, ER-Golgi			
YPT1	Suppressor	Suppressor	Suppressor
YKT6	Suppressor	Suppressor	Suppressor
BRE5	Suppressor	Suppressor	Suppressor
SEC21	Suppressor	Suppressor	Suppressor
UBP3	Suppressor	Suppressor	Suppressor
ERV29	Suppressor	Suppressor	Suppressor
SEC28	Suppressor	Suppressor	Suppressor
SFT1	Suppressor	Suppressor	Suppressor
GLO3	Enhancer	Enhancer	Enhancer
TRS120	Enhancer	Enhancer	Enhancer
GYP8	Enhancer	Enhancer	Enhancer
YIP3	Enhancer	Enhancer	Enhancer
BET4	Enhancer	Enhancer	Enhancer
SLY41	Enhancer	Enhancer	Enhancer
GOS1	Enhancer	Enhancer	Enhancer

Table S2. Cont.

Yeast gene	Effect with α-synFL	Effect with α-synΔ4	Effect with α-synΔ6
SEC31	Enhancer	Enhancer	Enhancer
Other cellular processes			
PFS1	Suppressor	Suppressor	Suppressor
PDE2	Suppressor	Suppressor	Suppressor
MUM2	Suppressor	Suppressor	Suppressor
OSH2	Suppressor	Enhancer	Enhancer
OSH3	Suppressor	Enhancer	Enhancer
PHO80	Suppressor	Suppressor	Enhancer
ISN1	Suppressor	Suppressor	Suppressor
EPS1	Enhancer	Enhancer	Enhancer
IDS2	Enhancer	Enhancer	Enhancer
TPO4	Enhancer	Enhancer	Enhancer
QDR3	Suppressor	Less enhancement	Less enhancement
IZH3	Enhancer	Enhancer	Enhancer
Newly characterized ORFs			
YKL088W (CAB3)	Suppressor	Suppressor	Suppressor
YDL121C	Suppressor	Suppressor	Suppressor
YBR030W (RKM3)	Suppressor	Suppressor	Suppressor
YOR129C (AFI1)	Suppressor	Suppressor	Suppressor
YOR291W (YPK9)	Suppressor	Suppressor	Suppressor
Unknown function			
YKL063C	Suppressor	Suppressor	Suppressor
YML081W (TDA9)	Suppressor	Suppressor	Suppressor
YNR014W	Suppressor	Suppressor	Suppressor
YML083C	Suppressor	Suppressor	Suppressor
YDR374C	Suppressor	Suppressor	Suppressor
YMR111C	Suppressor	Suppressor	Suppressor

The genes in this table were identified in refs. 1 and 2. Yellow highlighting marks effects that were different between FL a-syn and the splice isoforms.

1. Yeger-Lotem E, et al. (2009) Bridging high-throughput genetic and transcriptional data reveals cellular responses to alpha-synuclein toxicity. *Nat Genet* 41(3):316–323.
2. Cooper AA, et al. (2006) Alpha-synuclein blocks ER-Golgi traffic and Rab1 rescues neuron loss in Parkinson's models. *Science* 313(5785):324–328.